PROCEEDINGS OF SPIE

Highly efficient MIM diodes for NIR and SWIR applications

Elif Gul Arsoy, Emre Can Durmaz, Omer Ceylan, Meric Ozcan, Yasar Gurbuz

SPIE.

Highly Efficient MIM Diodes for NIR and SWIR Applications

Elif Gul Arsoy, Emre Can Durmaz, Omer Ceylan, Meric Ozcan, Yasar Gurbuz*

*Sabanci University, 34956, Orhanlı, Tuzla, Istanbul, TURKEY

yasar@sabanciuniv.edu

+90 216 483 9533

ABSTRACT

Metal-insulator-metal (MIM) diodes are highly considered in high frequency applications in form of rectennas for energy harvesting applications due to their fast speed, small size, and ease of fabrication and IC compatibility. In these diodes, insulators are integral part of the device, determining performance parameters. In this study, we have evaluated HfO_2 and Al_2O_3 based MIM diode structures to compare and determine performance parameters, with conversion efficiency being prioritized. The fabrication processes in physical vapor deposition (PVD) systems for the MIM diodes resulted in the devices having high non-linearity and responsivity. Also, to achieve uniform and very thin insulator layer atomic layer deposition (ALD) was used. We implemented the same MIM structure in 10x10 array form, with active area of 200x325 nm^2. The efficiency values of same arrays tested with 1200 and 1600 nm wavelength LEDs for 200x325 nm^2 diode active area without applying bias. The conversion efficiency value of the HfO_2 based structures calculated as 5% for 1200 nm wavelength. These measured values of conversion efficiency are reported for the first time in the literature for MIM diodes in SWIR operation.

Keywords: Metal-Insulator-Metal (MIM) diodes, quantum tunneling, IR harvesting and detection, rectennas.

1. INTRODUCTION

A metal-insulator-metal (MIM) diode consists of nanoscale insulator layer sandwiched between two metal layers. With the advancements in nanotechnology and fabrication capabilities, these devices have gained a lot of attention for variety of application areas such as infrared detection [1], energy harvesting optical rectennas [2]. The nano-scaled MIM diodes have further advantage of high speed quantum tunneling mechanism, enabling even THz regions of operation [3] and still rectify high frequency AC signal to DC. Due to the quantum nature of the rectification in such MIM diodes, photon assisted tunneling (PAT) theory [4] is applicable to calculate the optical response of these devices under a light illumination. The emitted or absorbed photons by electrons can tunnel through a barrier from initial state to final state. The absorbed incident radiation is rectified by MIM diode, generating DC current when AC input signal is applied to the devices under test. The barrier formation of the insulator between top and bottom metals in these devices allows tunneling assisted DC current [5].

In this work, we present nano-scaled MIM diodes, using two types of insulating layers to evaluate and compare their performance characteristics, such as I-V characteristics and responsivity. Moreover, the fabricated structures tested under LED illumination and without applying bias in order to calculate efficiency values. The devices are optimized for maximum conversion efficiency and compared using different insulator layers. The thickness of the insulator layer and the barrier formation are determinant for the tunneling current of MIM nano-diodes [6]. Barrier height of the devices, defined as difference of metal work function and electron affinity of the insulator layer parameters, are arranged to be small and also insulator layer is deposited with a thickness of a few nanometers, in order to increase tunneling current probability [7]. Fig. 1 is the illustration of a bias voltage effect and light illumination on barrier formation. Fig. 1(a) shows the barrier height formation of HfO_2 and Al_2O_3 insulator layers. Fig. 1 (a) presents change of barrier height under forward bias condition or light illumination of the $Au/Al_2O_3/Ni$ diode. Fig. 1 (b) shows barrier height formation and bias/light illumination effect on Cr-HfO_2-Ni MIM diode.
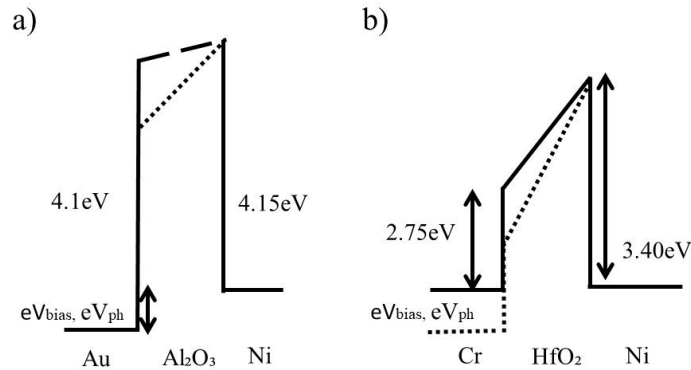
Fig. 1. Conduction band diagram of an asymmetric tunnel barrier with barrier height of the MIM structure in this study. For electrons at higher energy levels, tunneling probability increases. Work function of the Au and Ni are 5.1 eV and 5.15eV [8], respectively a) Fermi level shifting of the Au/Al_2O_3/Ni diode under applied dc bias voltage or light illumination condition. The shift of the left side Fermi level is equal with the eV_{bias} or eV_{photon} where V_{photon} equals to $h\omega/e$. b) Asymmetric barrier formation, barrier thickness and height tunability of the Cr/HfO_2/Ni MIM structure with the change of applied DC bias voltage or light illumination condition.Work function ot the Cr is 4.5 eV [8] and electron affinity value of the HfO_2 is 1.75 eV [9]. The barier height between top metal, Ni and the insulators Al_2O_3 and HfO_2 are 4.15eV and 3.40 eV respectiveley.

The response of the MIM devices to light illumination changes with respect to the insulator layer since the barrier height is a key impact on tunneling probability when the thickness of the insulator layer is thin enough for the tunneling [10]. For instance, if the barrier height between the insulator layer and the metal is considerably high, the tunneling probability is relatively low since tunneling distance of electrons becomes longer. However, tunneling distance of the electrons gets shorter under the illumination due to the barrier asymmetry. Therefore, the current difference due to illumination, in other words response of the devices under the illumination, increases. Fig. 1 presents the illumination effects, barrier height comparison in terms of photon generated current and response and the effect of the asymmetry between top and bottom metal.

2.   DESIGN AND FABRICATION

The MIM diodes are fabricated on top of the highly resistive ($>10^8$ Ω.cm) GaAs substrate. For the first devices, bottom metal is selected as Au and Ni is used as a top metal. In second device's fabrication process, the insulator layer is HfO_2; Cr and Ni are used as bottom and top metals, respectively. Cr/HfO_2/Ni formation is selected due to the fact that HfO_2 is a promising material for several applications, with its IC compatible and thermodynamic stable characteristics [11]. The asymmetric barrier formation allows high quantum tunneling. The metal and the insulator thicknesses are 100 nm and 1.5 nm, respectively. E-beam lithography is employed to pattern the nano-lithographic features on the PMMA resist, followed by a thermal deposition of metal layers and Atomic Layer Deposition (ALD) of the insulator layer. Atomic Layer Deposition precursor of HfO_2 is tetrakis (dimethylamido)Hafnium (Hf(NMe$_2$)$_4$) fulfilled at 100 C , trimethylaluminum (TMA) for Al_2O_3 at 80 C. SEM images of the samples consisted of Cr/HfO_2/Ni, as the representative of the MIM structures in this study, is presented in Fig. 2(a), along with cross-sectional view illustration of the devices. Fig. 2(b) represents 10x10 array of Cr/HfO_2/Ni MIM structure with an inset of focused view.
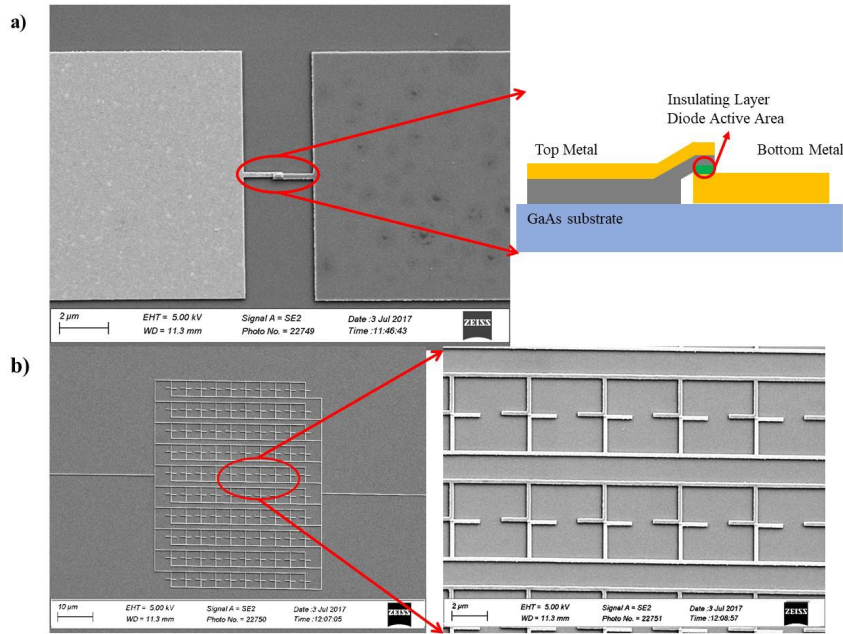
Fig. 2. SEM images of the MIM structure a) single b) 10x10 array format.

In general terms, the efficiency of such devices is the ratio of useful output power to consumed input power. For our application, the efficiency can be described as the ratio of output electrical power (DC) to incident optical radiation power (η) given in equation (1).

$$\eta = \frac{P_{Output}}{P_{Input}} = \frac{P_{Output}^{DC}}{P_{Optical}}$$

(1)

$$\eta = \frac{P_{Output}^{DC}}{Incident\ Radiation\ Intensity\ x\ Collector\ Area}$$

The photon generated current as a result of PAT and photon generated current is transferred to a load to obtain external electrical power from device, as shown in Fig.3. The reason of using a load is to calculate the efficiency of the devices from the measured data. The measurements for the efficiency calculation are performed under zero bias condition in order to separate the DC bias effect from photon generated current. Since the fabricated structures are in nano-scale, integration of the load resistance with the fabricated MIM structures and transfer of the photon generated current from device to output are difficult. To overcome these difficulties, we designed a custom measurement system that consists of the isolated cables, connectors and a load resistance in an isolated box, as presented in Fig 3.
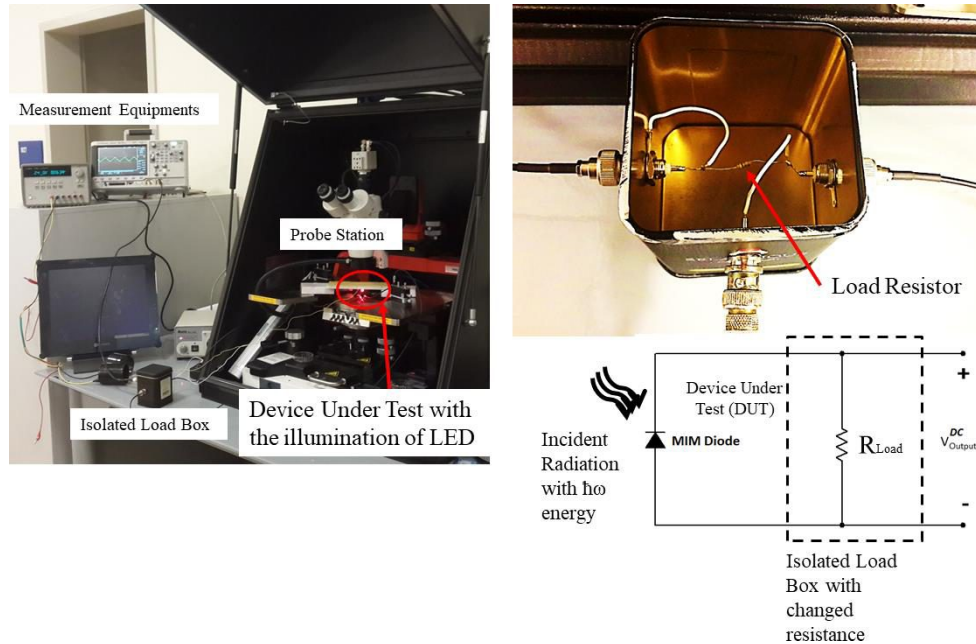
Fig. 3. Test setup of MIM structures under illumination without applying bias. V_{Output}^{DC} is measured by using multimeter as a result, output power transfer is calculated.

3. RESULTS

DC characterizations of the MIM structure are carried out by using Agilent B1500A Semiconductor Parameter Analyzer. The IV measurements are taken by applying DC bias voltage to DC pads of the device via DC probes, in a dark environment, generated in the shielded probe station. The transient results of the fabricated structures are shown in Fig. 4. Then, we have placed with 1200 and 1600 nm wavelength LEDs, with controlling the power of the LEDs by changing the current without applying bias to obtain photon generated current, inside the probe station on top of the device under test which is the $Cr/HfO_2/Ni$ structure.

The fabricated devices have different resistance value due to the different insulator layers and to evaluate the efficiency comparably, load resistance is fixed as a constant 5 MΩ since the resistance of the fabricated devices are in less than the 10 MΩ range. Moreover, the incident radiation intensity is measured with Newport Dual Channel Power Meter 2832-C. The collector area is assumed, for our calculations, to be directly the active area. For the array format the active area is multiplied with the total element number, 100 (10x10 array size). The efficiency values of the HfO_2 based devices for different illumination sources are shown in Table II.

TABLE II
EFFICIENCY MEASUREMENT RESULTS FOR 10X10 MIM ARRAY WITH 200X325 nm²

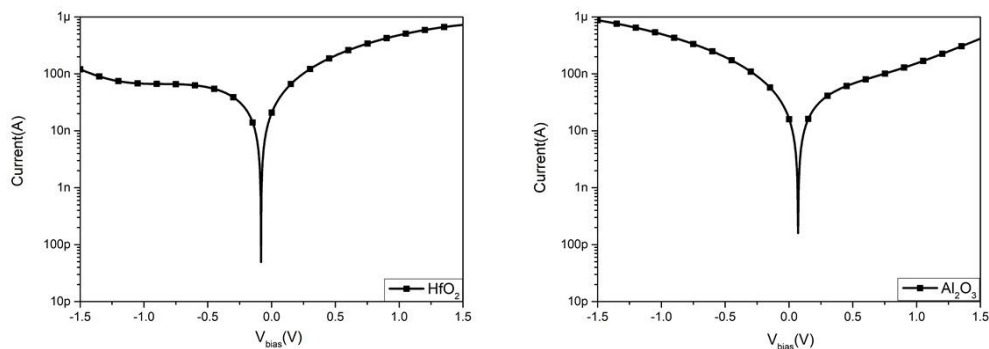| Illumination source	Voltage across 5 MΩ Load Resistance (mV)	Output Power (pW)	Incident Radiation Flux (mW/cm²)	Efficiency (%)
1200 nm LED	5.2	5.4	1.5	5
1600 nm LED	1.5	0.45	0.65	1

Fig. 4. IV characteristics of the Cr/HfO$_2$/Ni and Au/Al$_2$O$_3$/Ni, respectively.

4. CONCLUSION

In this work, MIM diodes with different materials are fabricated on the GaAs substrate. We have evaluated 2 different insulator materials (HfO$_2$ and Al$_2$O$_3$) in MIM diode structures to compare, determine performance parameters. Moreover, structures tested under different illumination sources and efficiency values of the samples calculated by using load resistance and without applying bias. The fabricated MIM structures show non-linear characteristics. Moreover, photo-generated current obtained under illumination without applying bias. The efficiencies of the devices were varying with the material type and the wavelength of the source. The sizes of the devices are small enough to ease integration with IC's. These results show that the MIM structures have sufficient potential to be used in applications of IR detection and harvesting.

ACKNOWLEDGMENT

REFERENCES

[1] I. Azad, M. K. Ram, D. Y. Goswami, and E. Stefanakos, "Au/Cr-ZnO-Ni structured metal-insulator-metal diode fabrication using Langmuir-Blodgett technique for infrared sensing," Infrared Technol. Appl. XLII, vol. 9819, p. 98190E, 2016.

[2] E. G. Arsoy, M. Inac, A. Shafique, M. Ozcan, Y. Gurbuz, " The metal-insulator-metal diodes for infrared energy harvesting and detection applications", Proc. SPIE, vol. 9819, 2016.

[3] E. I. Hashem, N. H. Rafat, E. A. Soliman, "Theoratical Study of Metal-Insulator-Metal Tunnelling Diode Figures of Merit," IEEE Journal of Quamtum Electronics, vol. 49, no.1, pp. 72-79, 2013.

[4] S. Joshi and G. Moddel, "Optical rectenna operation: where Maxwell meets Einstein," J. Phys. D. Appl. Phys., vol. 49, no. 26, p. 265602, 2016.

[5] F. Yesilkoy, "IR Detection and Energy Harvesting using Antenna Coupled MIM Tunnel Diodes , PhD Dissertation , 2012 Professor Martin Peckerar," p. 160, 2012.

[6] S. Grover and G. Moddel, "Engineering the current-voltage characteristics of metal-insulator-metal diodes using double-insulator tunnel barriers," Solid. State. Electron., vol. 67, no. 1, pp. 94–99, 2012.

[7] G. Moddel and S. Grover, "Rectenna solar cells," Rectenna Sol. Cells, vol. 9781461437, no. Mim, pp. 1–399, 2013.

[8] H. B. Michaelson and H. B. Michaelson, "The work function of the elements and its periodicity The work function of the elements and its periodicity," vol. 4729, no. 1977, pp. 1–6, 2013.

[9] S. Monaghan, P. K. Hurley, K. Cherkaoui, M. A. Negara, and A. Schenk, "Solid-State Electronics Determination of electron effective mass and electron affinity in HfO$_2$ using MOS and MOSFET structures," Solid State Electron., vol. 53, no. 4, pp. 438–444, 2009.

[10] L. Li, "Study of Metal-Insulator-Metal Diodes for Photodetection," 2013.

[11] R. L. N. I et al., "Thermal and Plasma-enhanced Atomic Layer Deposition of hafnium oxide on semiconductor substrates #," pp. 112–115.